ACS OMEGA

http://pubs.acs.org/journal/acsodf

Article

Nucleophilic Regulation of the Formation of Melanin-like Species by Amyloid Fibers

Daehong Ha and Kyungtae Kang*

Cite This: *ACS Omega* 2022, 7, 773−779

Read Online

ACCESS | Metrics & More | Article Recommendations | Supporting Information

ABSTRACT: This work examines the influences of amyloid fibers of hen egg white lysozyme (HEWL) on the formation of melanin-like species (MLS) with a rationally selected set of catechol derivatives. Catechol−amyloid interactions, which are central in melanogenesis, are complex and multifaceted, making them difficult to understand at the molecular level. The catechol derivatives are set to interact with HEWL amyloid fibers upon altering pH, and the resultant formation of MLS is characterized. For obtaining clues for the molecular mechanism by which HEWL fibers regulate the formation of MLS, putative intermolecular interactions are individually perturbed and their ramifications are analyzed. With the entire data set, we could conclude that the externally presented nucleophilic moieties of HEWL fibers play a major role in regulating the material and kinetic properties of MLS and their formation, respectively.

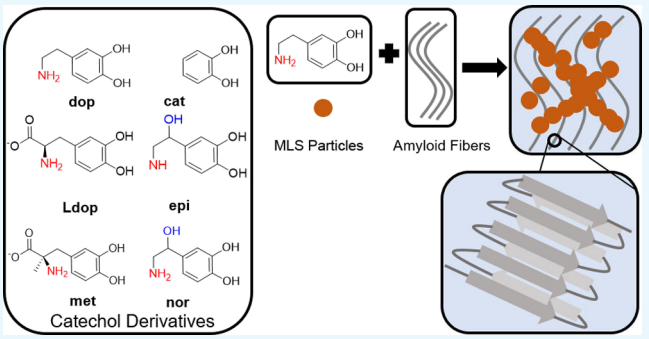

INTRODUCTION

Catechol derivatives (broadly encompassing catechols, catecholamines, and flavonoids) have been frequently linked to amyloid—a protein-aggregated fibrillar structure rich in cross-β-sheets—and its related diseases as a potential cure. Many compounds [e.g., dopamine (DA)/L-dopa (LD),[1,2] flavonoids,[3] and polyphenols[4,5]] were reported effective in morphologically remodeling amyloid fibers or in altering the kinetics of their formation. One remarkable example is epigallocatechin-3-gallate (a major component in green tea extracts), which is currently involved in multiple clinical trials for its activities in remodeling amyloid fibrillar structures and neutralizing their cytotoxicity.[6,7] The molecular mechanism by which catechol derivatives regulate various features of amyloid fibers is still vague, except a few clues implying that it relies on a combination of multiple intermolecular interactions, and that it largely depends on the context.[8] More recent efforts on elucidating the relationship between catechol derivatives and amyloid aggregation, however, were relatively rare, presumably because the causality between the amyloid species and the onset of neurodegenerative diseases is being challenged these days.[9]

Nevertheless, understanding catechol−amyloid interactions may have diverse implications other than those only related to combating amyloid diseases. The nature of catechol−amyloid interaction is beyond a simple unilateral regulation of one by another, but it is mutual and multifaceted. Under oxidative conditions, catechol derivatives (particularly catecholamines) spontaneously form heterogeneous molecular complexes—often called "melanin-like species (MLS)"—composed of non-covalently associated oligomeric structures.[10,11] Interestingly, such oxidative association of catechol derivatives may be regulated critically by amyloid fibers. In melanogenesis (i.e., the oxidative association of DA), amyloid fibers made of a melanosomal protein (Pmel17) play central biochemical roles.[12−15] Genetically removing Pmel17 causes losses of pigmentation and melanocytes.[16] A currently accepted role of Pmel17 fibers is capturing toxic intermediates during the process of melanogenesis, but their actual role is likely multifaceted and underestimated. We have previously shown that amyloid fibers made of various proteins [subdomains of Pmel17 and even a biologically irrelevant protein, hen egg white lysozyme (HEWL)] have multiple functions on the oxidative association of DA,[17] such as accelerating the formation of MLS and altering their morphological and material properties greatly. This indicates that the supramolecular structure of amyloids, but not solely their amino acid sequences, enables them to interact with catechol derivatives.

Taken together, amyloidogenic proteins and catechol derivatives have complex and mutual interactions, particularly regarding the supramolecular association of one another. The molecular mechanism—and even the presence of—these

Received: September 29, 2021
Accepted: December 7, 2021
Published: December 20, 2021

https://doi.org/10.1021/acsomega.1c05399
ACS Omega 2022, 7, 773−779

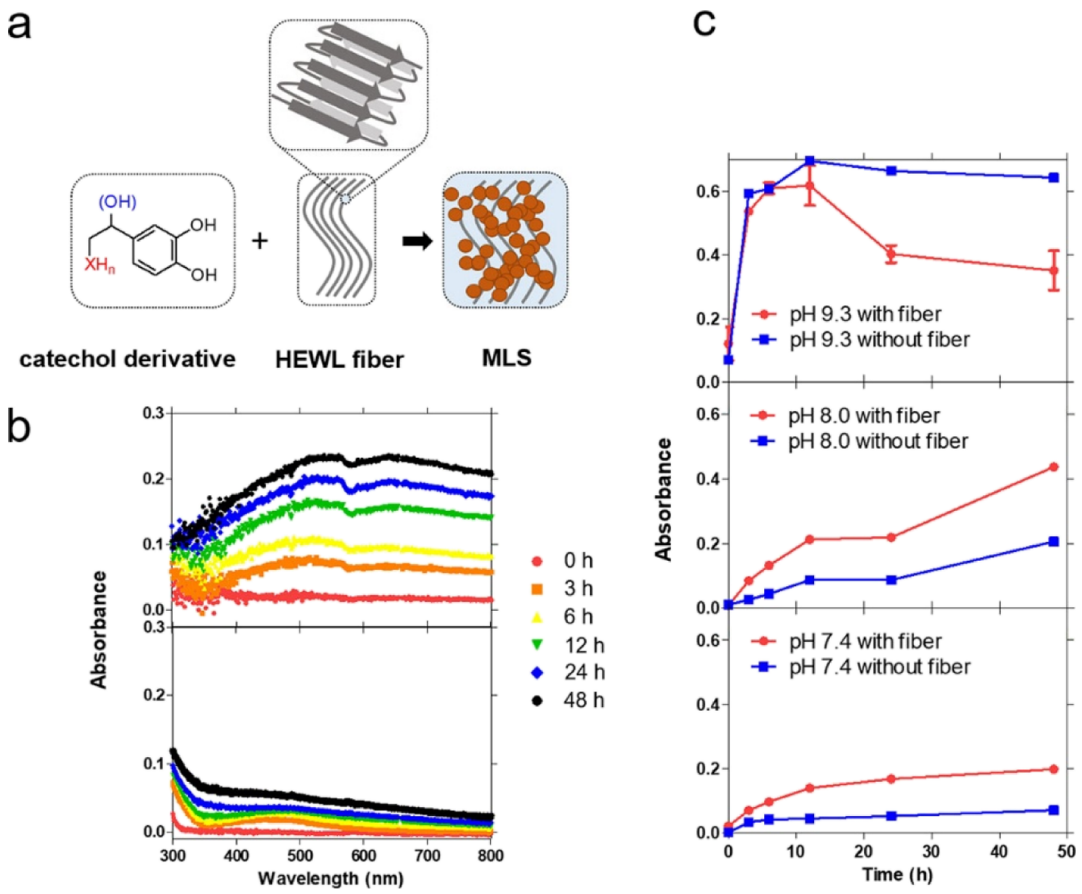

Figure 1. (a) Schematic illustration of the amyloid-templated formation of MLS. (b) Absorbance spectra of a solution of dopamine (250 μM) and HEWL fibers (20 μM) after 0, 3, 6, 12, 24, and 48 h of incubation (above) with and (below) without HEWL fibers. (c) Temporal changes of the A_{450} values of solutions of (a) at pH 7.4, pH 8.0, and pH 9.3.

mutual interactions remain incompletely considered. Particularly, there has been no fundamental approach to reveal how amyloid fibers regulate the oxidative association of catechol derivatives despite its direct relevance to melanogenesis. Understanding amyloid−catechol interactions would also provide clues for discovering emergent chemical functions of various functional amyloids—amyloids designed by nature to have desired chemical/material functions.[18] In this work, we sought to elucidate the molecular-level roles of amyloid fibers in the oxidative association of various catechol derivatives by using HEWL fibers as a representative amyloid structure (Figure 1a). The ramifications of varying the molecular structures of catechol derivatives and HEWL fibers, or the reaction conditions and the ramifications of varying were carefully analyzed. Material/chemical properties of the MLS formed under different conditions were examined using spectroscopic and micrographic methods.

METHODS

Materials. DA, methyl L-dopa (MD), epinephrine (EP), norepinephrine (NE), and acetic anhydride were purchased from Sigma-Aldrich. Catechol (CA) and LD were purchased from Alfa Aesar. HEWL was purchased from Thermo Fisher. Hexanediol and NH_4Cl were purchased from Daejung Chemicals & Metals. NMe_4Cl was purchased from Samchun Pure Chemical. The transmission electron microscopy (TEM) grid was purchased from Electron Microscopy Sciences.

Preparation and Quantification of HEWL Amyloids. HEWL was dissolved in a solution of potassium phosphate buffer (20 mM; pH 6.3) containing 2 M of GdnHCl to a concentration of 2 mg/mL. The concentration of HEWL was measured based on the absorbance at 280 nm using an Eppendorf BioPhotometer D30 (extinction coefficient of HEWL: 38 904 M^{-1} cm^{-1}). The solution of HEWL was then incubated at 60 °C with a vigorous and continuous stirring for 4 h. As the reaction progressed, the HEWL solution became turbid. The solution was centrifuged three to five times at 12 000 rpm to remove remaining salts and monomeric HEWL from the solution. In between each centrifugation, the supernatant was discarded and the same volume of distilled water was added. Here, the concentrations of monomeric HEWL in each discarded supernatant were measured, which were then subtracted from the initial concentration of HEWL to give the concentration of HEWL fibers finally synthesized.

Formation of MLS from Various Catechol Derivatives. An aqueous solution (250 μM) of each catechol derivative at a desired pH was added to a solution of HEWL fibers (20 μM). Potassium phosphate buffer (20 mM) was used for pH 7.4 and pH 8.0, and carbonate-bicarbonate buffer (20 mM) was used for pH 9.3. The volume of the solutions was set to 2 mL in cuvettes, with a continuous shaking by an agitator (200 rpm). The absorbance at 450 nm was measured after 0, 3, 6, 12, 24, and 48 h of their incubation.

Acetylation of Lysozyme Fibrils. Acetic anhydride (0.047 mL for 1 g of HEWL fiber) was added to a solution

https://doi.org/10.1021/acsomega.1c05399
ACS Omega 2022, 7, 773−779

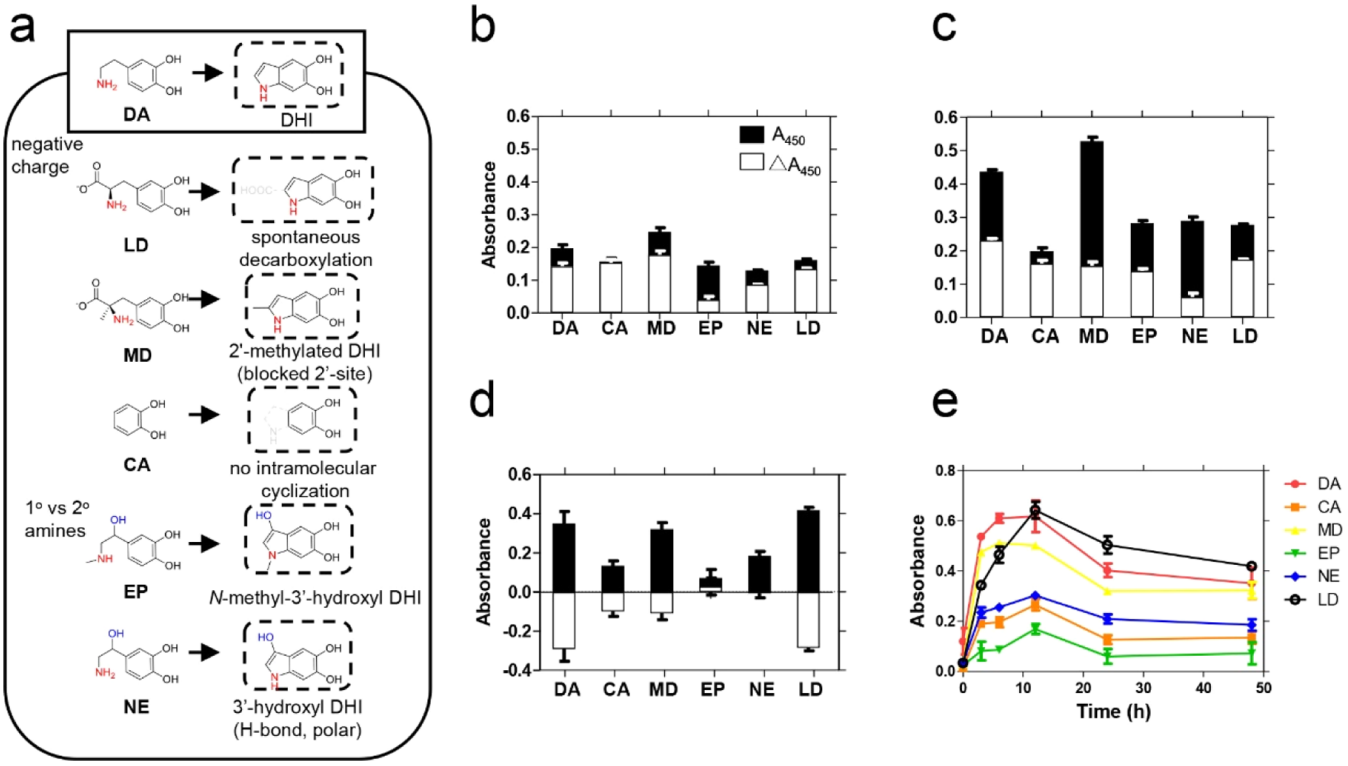

Figure 2. (a) Catechol derivatives used in this work and the reasons why they were selected. (b–d) A_{450} and ΔA_{450} values of samples containing each catechol derivative after 48 h of incubation at (b) pH 7.4, (c) pH 8.0, and (d) pH 9.3. (e) Gradual decrease of A_{450} values of solutions containing MLS of each catechol derivative and HEWL fibers at pH 9.3.

of HEWL fibers (pH 8.0) and stirred for 2 h at room temperature. The resultant fibers were collected by centrifugation three times.

Fourier-Transform Infrared Spectroscopy. Solutions containing fibers and/or catechol derivatives at desired time points were centrifuged at 12 000 rpm for 10 min and were lyophilized. The dried sample was then analyzed by using a Spectrum One System (Perkin-Elmer).

TEM. For TEM analysis, solutions containing samples were desalted by repetitive washing with distilled water. Each sample was adsorbed onto a Formvar/carbon-coated copper grid for 3 min, then washed several times with distilled water and dried. The grids were stained with a solution of sodium phosphotungstate (0.6 mM) for 5 min, before they were washed and dried in air. The samples were analyzed using a JEM-2100F.

RESULTS AND DISCUSSION

Incubation of DA in a basic environment (pH 8.0–8.5) greatly accelerates its oxidative association. When Tris buffer is used as a solvent, a basic environment (pH 8–8.5) leads to the surface-independent formation of an organic thin film (often called "polydopamine").[19] Under more basic conditions (at pH higher than 9.0), however, MLS are known to disassemble likely due to the deprotonation of amine groups.[20] Given that pH is a crucial factor in the formation of MLS, we asked how the influences of HEWL fibers on the formation of MLS vary upon altering pH. The formation of MLS is easily confirmable by observing broad monotonic light absorption in the ultraviolet–visible range as previously reported. The presence of HEWL fibers (250 μM of DA; 20 μM of HEWL fibers; the concentrations were chosen based on our previous results[17]) clearly accelerated the formation of MLS at pH 7.4, consistent with our previous results (Figure 1b). Based on the observed monotonic light absorption, we used absorbance at 450 nm (A_{450}) as a quantitative measure for the amount of MLS and examined their formation at multiple pH values in the presence and absence of HEWL fibers (Figure 1c). Increasing pH resulted in the general increase of MLS synthesized without HEWL fibers, but such a trend was not consistent in the presence of HEWL fibers. At pH 9.3, remarkably, HEWL fibers resulted in a gradual decrease of the MLS after 12 h (Figure 1c). This gradual decrease was not observed without HEWL fibers, indicating that HEWL fibers acted adversely to the stability of MLS at this pH.

The formation of MLS is a multistep oxidative self-association of a catechol derivative. The molecular components and the formation process of MLS are incompletely understood due to their complex nature. One of the key steps in the association process is the formation of 5,6-dihydroxyindole (DHI), which has a planar and aromatic structure with a stable radical character. DHI is synthesized by intramolecular Michael-type cyclization between quinone and amine groups, and it is subsequently oligomerized via radical-dependent pathways. To examine the formation of MLS and influences of HEWL fibers therein, we chose a series of catechol derivatives (DA, LD, MD, CA, EP, and NE), with the following rationales (Figure 2a): (i) CA does not have an amine group to undergo intramolecular cyclization; (ii) LD contains an additional negatively charged carboxyl group, (iii) MD is a methylated version of LD, which forms 2′-methylated DHI upon oxidation; (iv) EP and NE have an additional hydroxyl group, providing a hydrogen bonding site. Measured redox properties (Figure S1) and pK_a values (Figure S2) of the

https://doi.org/10.1021/acsomega.1c05399
ACS Omega 2022, 7, 773–779

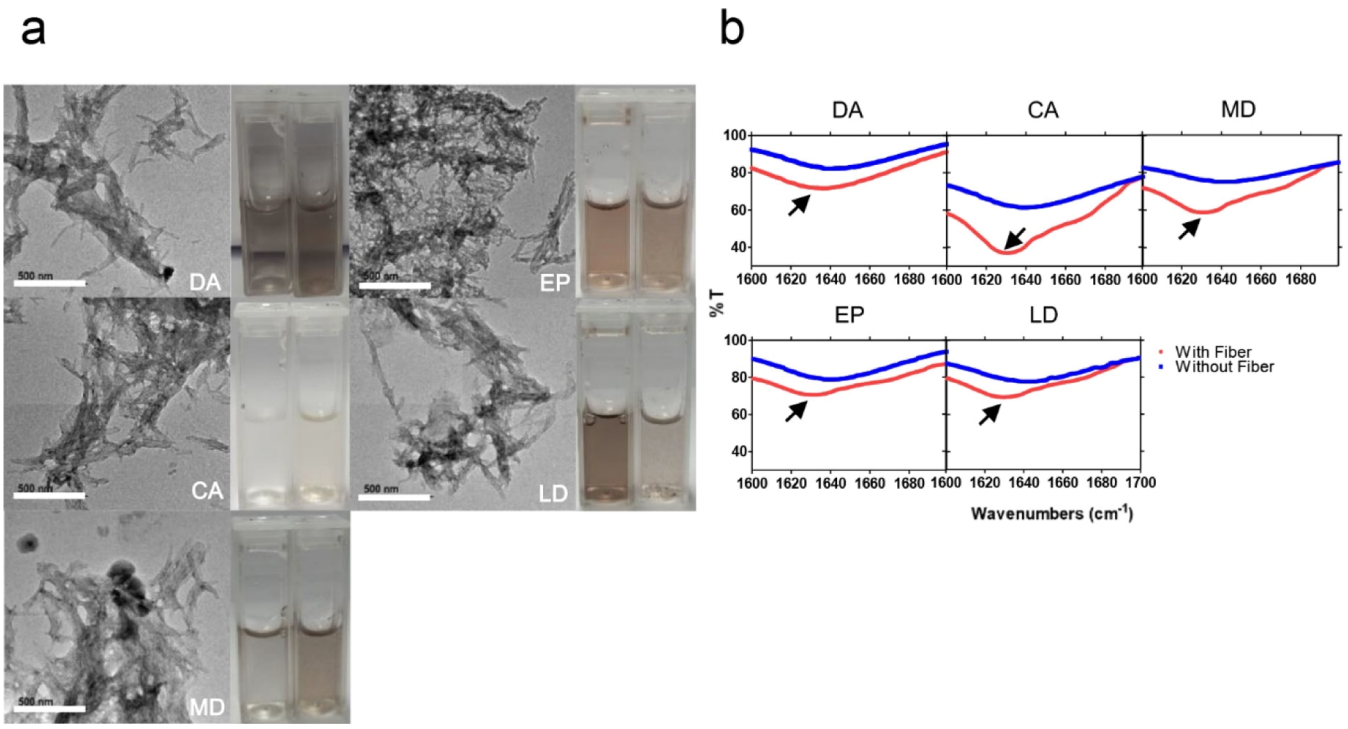

Figure 3. (a) TEM images and digital photographs of various MLS synthesized with (right cuvettes) or without (left cuvettes) HEWL fibers at pH 8.0 after 24 h. (b) FT-IR spectra of MLS formed from DA, CA, MD, EP, and LD with and without fiber at pH 8.0. The arrows show peaks indicative of β-sheet components.

catechol derivatives were comparable with each other, suggesting that their initial oxidation is chemically similar. Figure 2b–d shows the values of A_{450} and differences in those upon addition of HEWL fibers (ΔA_{450} = A_{450} of MLS with HEWL fibers—A_{450} of MLS without HEWL fibers) after 48 h under each condition. As in the case of DA, oxidative association of the catechol derivatives was facilitated when increasing pH. The values of ΔA_{450}, however, did not follow the pH-dependent increasing trend of A_{450} for all the catechol derivatives tested. The values of ΔA_{450} barely changed between pH 7.4 and 8.0, and turned negative in pH 9.3, as observed in the case of dopamine (Figures 2b–d and S3). Like the case of DA, addition of HEWL fibers at pH 9.4 caused an initial increase of values of A_{450}, followed by their gradual decrease for all the catechol derivatives tested (Figure 2e). The observed discrepancy between trends of ΔA_{450} and A_{450} upon pH alteration indicates that the HEWL fibers primarily interact with only a subset of molecular structures—which are likely common in all the catechol derivatives—among which appear the process of oxidative association. The adverse activity of HEWL fibers on MLS at pH 9.3 implies that the positive charge of externally presented lysine residues of HEWL fibers (the pK_a value of whose conjugate acid is about 10, but it may be lower in a physically confined space as the surface of fibers) is crucial for the stability of the HEWL–MLS composite.

Despite the comparable pH-dependency, the kinetics of the formation of MLS differed critically among catechol derivatives. Remarkably, MD showed the highest value of A_{450} at lower pH (7.4 and 8.0). MD and LD, which have similar molecular structures, were distinguishable in the kinetic features of their association processes. This reflects that 2′-methylated DHI (which is expected to form after oxidation of MD) is more favorable to oxidative association than DHI; the carboxyl groups in LD and MD are prone to spontaneous decarboxylation during multiple stages of oxidation and tautomerization (Figure 2a). A previous work suggested that the 2′ position of DHI plays a deterministic role in the antioxidant property of melanin because it may prevent the formation of linearly aligned 4,7-linked DHI oligomers.[21] The values of ΔA_{450} for MD, however, remained similar to (or slightly decrease from) those of DA and LD, which implies that HEWL fibers do not primarily interact with DHI-related compounds species. This is further supported by the fact that the values of ΔA_{450} of CA, which is unable to cyclize into DHI, were again similar to those of DA and LD at lower pH. The total amount of MLS (i.e., A_{450}) formed from CA was much smaller than those formed from other catechol derivatives. EP and NE showed the lowest values of A_{450} and ΔA_{450} over all the pH range, indicating that the 3′-hydroxyl group impedes simultaneously their oxidative association and their interaction with HEWL fibers. The suppressed association kinetics of NE is in line with a previous report that showed a thinner but more uniform coating of polynorepinephrine compared to polydopamine.[22] Such trends of the formation of MLS among the catechol derivatives remained consistent when their concentrations were significantly increased (Figure S4).

Next, we examined influences of HEWL fibers on material properties of MLS synthesized from the catechol derivatives. Figure 3a shows the transmission electron micrographs of various MLS in the presence [or absence (Figure S7)] of HEWL fibers. The images show that HEWL fibers are embedded within dark and amorphous MLS and bundled together to form larger composite structures, regardless of which catechol derivative was used. MLS composited with HEWL fibers were easily dispersible in an aqueous solution by a brief vortexing, whereas those without strongly adhered to the cuvette (Figure 3a). Fourier-transform infrared (FT-IR)

https://doi.org/10.1021/acsomega.1c05399
ACS Omega 2022, 7, 773–779

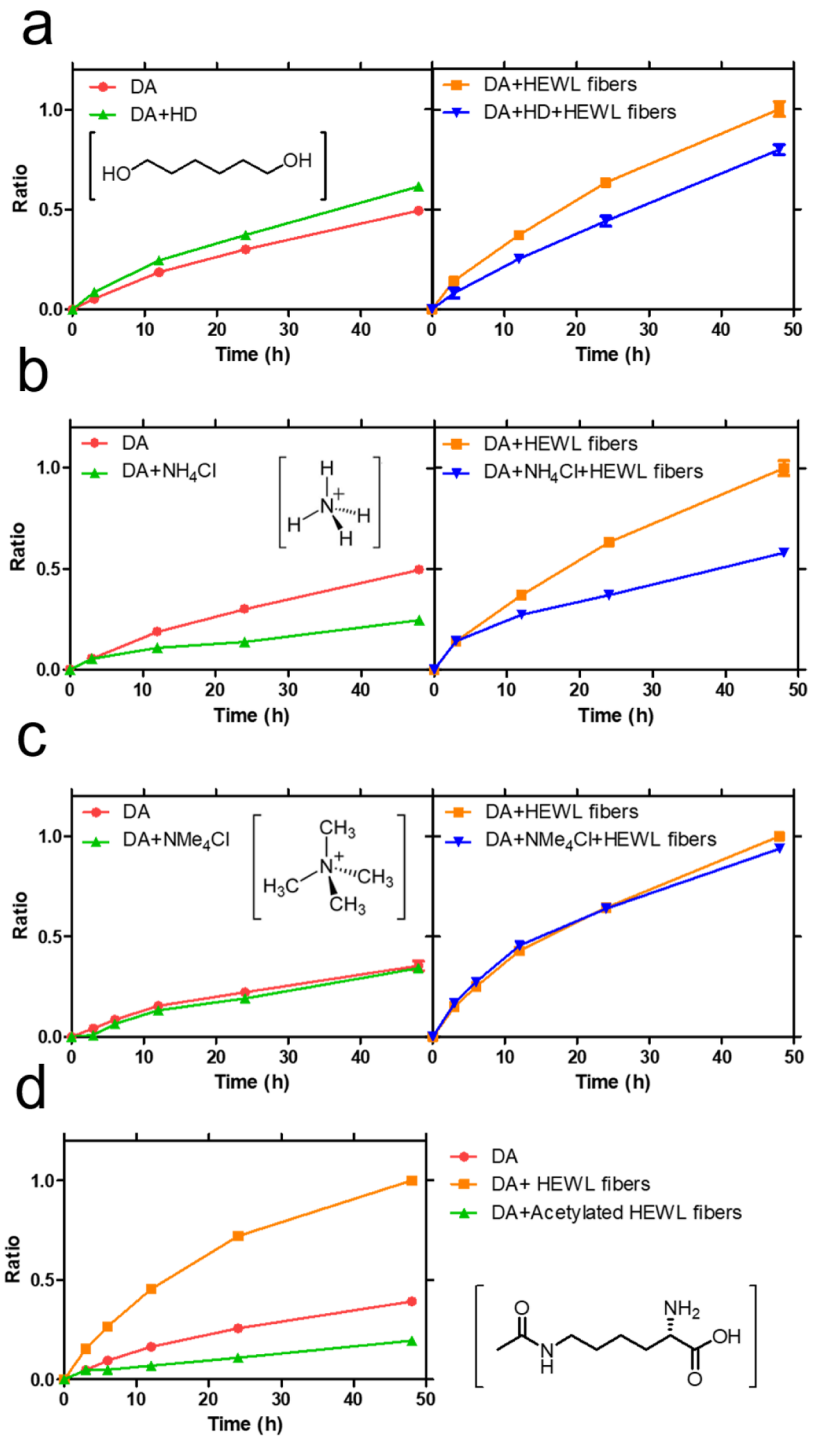

Figure 4. (a–c) A_{450} values of MLS formed from DA with and without HEWL fibers in the presence of (a) HD, (b) NH_4Cl, and (c) NMe_4Cl at pH 8.0 after 48 h. (d) A_{450} values of MLS formed from DA, DA with HEWL fibers, and DA with acetylated HEWL fibers. All the values were normalized with respect to those with HEWL fibers at 48 h for each set.

spectroscopy also confirmed the presence of parallelly aligned β-sheet structures (~1630 cm^{-1}) in MLS composited with HEWL fibers, indicating that the amyloid structure was not remodeled or decomposed during the process of the oxidative association (Figure 3b). These results indicate that amyloid fibers are capable of critically regulating physical properties (e.g., morphology, water-disposability, and supramolecular configuration) of the resultant MLS for a broad range of catechol derivatives.

To further investigate the molecular mechanisms by which HEWL fibers regulate the oxidative association of the catechol derivatives, we tried to individually perturb putative intermolecular interactions between fibers and catechol derivatives. We expected the most probable role of HEWL fibers to be recruiting catechol derivatives by an attractive interaction because HEWL has no redox-active moieties. Such a recruitment would accelerate the O_2-dependent spontaneous oxidation of a catechol derivative and its further accumulation. Given that interactions between amyloids and catechol

https://doi.org/10.1021/acsomega.1c05399
ACS Omega 2022, 7, 773−779

derivatives are multifaceted and complicated, we suspected that the mechanism would be a combination of multiple molecular interactions. Previous studies focusing on the capability of catechol derivatives for remodeling amyloid fibers have provided us a few strong candidates to start with: (i) hydrophobic interactions, (ii) cation−π or electrostatic interactions (amyloids and oxidized forms of catechol derivatives both contain charged moieties and aromatic systems simultaneously), and (iii) the formation of a Schiff base between externally exposed lysine residues of amyloid fibers and quinone intermediates. We chose DA and pH 8.0 as standard conditions under which the role of each molecular interaction in the regulatory functions of HEWL fibers was studied.

To examine the influences of hydrophobic interactions, we added 1,6-hexanediol (HD), which is known to interfere strongly with hydrophobic interactions. Addition of a large amount of HD (500 mM) partially attenuated the influence of HEWL fibers in the formation of MLS; HEWL fibers (20 μM) increased the amount of MLS synthesized 2.02-fold at 48 h, but with HD, the increase became 1.61-fold (Figure 4a). At the same time, however, addition of HD facilitates the formation of MLS in the absence of the fibers (∼1.24-fold). Therefore, addition of excess HD likely overrode the catalytic influences of HEWL fibers with its own activity in regulating the formation of MLS. Most of the molecular intermediates during the formation of MLS are planar and aromatic and thus their association would be largely influenced when the hydrophobicity of the reaction environment is altered. The results overall indicate that both the formation of MLS and the regulatory functions of HEWL therein, at least partially, rely on hydrophobic interactions.

Next, we added an excess amount of an ammonium (NH_4Cl) or a tetramethyl ammonium (NMe_4Cl) salt to the reaction mixture, to examine the role of cation-driven molecular interactions in the observed regulating properties of HEWL fibers. Both cations have a positive charge, while only NH_4^+ can lose a proton and act as a weak nucleophile depending on the local chemical environment. Addition of an excess amount of NH_4Cl (500 mM) attenuated the formation of MLS (Figure 4b) at 48 h. The influence was consistent regardless of the presence of HEWL fibers, indicating that the added salts acted adversely on the general process of the oxidative association, rather than specifically on the interactions between them and HEWL fibers. This trend stayed consistent when lower concentrations of NH_4Cl were added (Figure S5), but disappeared when the pH was lowered to 7.4 (Figure S6). In contrast, addition of NMe_4Cl (500 mM) did not bring about a noticeable change in the formation of MLS regardless of pH and the presence of HEWL fibers (Figures 4c and S6). This indicates that, in contrast to our initial assumption, cation−π and electrostatic interactions do not play a deterministic role in the formation of MLS under our experimental conditions. Cation−π interactions between oligomeric species of quinone derivatives have been suggested as the major driving force in the formation of a polydopamine thin film (at the solid−liquid interface).[20] Our results, however, suggest that their influences are marginal in the solution-dispersed phase. The observed influence of NH_4Cl, thus, likely arose from the nucleophilic property of its deprotonated form. The deprotonated form of NH_4^+ can form a Schiff base with carbonyl groups or undergo Michael-type addition to DHI derivatives, interfering reactions of other amines.

Assuming the nucleophilic moieties being important in the interaction between catechol derivatives and HEWL fibers, we conducted acetylation of HEWL fibers to modify externally presented Lys (and possibly Cys) of HEWL fibers, neutralizing their nucleophilicity. Acetylation was performed according to the previously described method.[23] As shown in Figure 4d, acetylation completely abolished the influences of HEWL fibers on the formation of MLS. When all the results of Figure 4 are combined, we could conclude that the interactions between the catechol derivatives and HEWL fibers are a combination of hydrophobic interactions and covalent interactions relying on the nucleophilicity of lysine residues in HEWL fibers, while the latter plays a primary role. Lys residues have also been suspected as a major mediator in the flavonoid-based inhibition of amyloid-β aggregation.[24]

In summary, we examined the role of HEWL amyloid fibers in the formation of MLS by using a rationally selected set of catechol derivatives. Regardless of the molecular structure, the formation of MLS was commonly facilitated by HEWL fibers to different extents for each catechol derivative. HEWL fibers also critically regulated the morphological and material properties of various MLS. By individually perturbing relevant intermolecular interactions, we concluded that the externally presented nucleophilic moieties of HEWL fibers likely play a major role in regulating the formation of MLS. We believe that this work merits considering amyloid structures as a natural way of designing supramolecular functionality, rather than merely a pathological hallmark. Increasing evidence reveals biological contexts in which amyloids are intentionally designed and synthesized by the host organisms, such as forming adhesive biofilms,[25,26] regulating homeostasis,[27] obtaining antimicrobial properties,[28] storing hormones,[29] and regulating amyloid pathogenesis.[30,31] Investigating the chemical aspects of such functional amyloids would be crucial for engineering amyloid structures as biomaterials and for understanding the chemical origin of their biological influences (either beneficial or detrimental).

■ ASSOCIATED CONTENT

Supporting Information

The Supporting Information is available free of charge at https://pubs.acs.org/doi/10.1021/acsomega.1c05399.

Cyclic voltammograms and pK_a values of the catechol derivatives and supplementary data for kinetic and mechanistic analyses of MLS formation in the presence of HEWL fibers (PDF)

■ AUTHOR INFORMATION

Corresponding Author

Kyungtae Kang − *Department of Applied Chemistry, Kyung Hee University, Yongin 17104, South Korea;* orcid.org/0000-0003-4236-8922; Email: kkang@khu.ac.kr

Author

Daehong Ha − *Department of Applied Chemistry, Kyung Hee University, Yongin 17104, South Korea*

Complete contact information is available at: https://pubs.acs.org/10.1021/acsomega.1c05399

https://doi.org/10.1021/acsomega.1c05399
ACS Omega 2022, 7, 773−779

Author Contributions

D.H. and K.K. wrote the manuscript. K.K. designed the research. D.H. collected the experimental data.

Notes

The authors declare no competing financial interest.

■ ACKNOWLEDGMENTS

This work was supported by the National Research Foundation of Korea (NRF) grant funded by the Ministry of Science, ICT & Future Planning (MSIP) (2019R1C1C1009111 and 2021R1A4A1030449) and the GRRC program of Gyeonggi province [GRRC-kyunghee2017(A01)].

■ ABBREVIATIONS

HEWL, hen egg white lysozyme; MLS, melanin-like species; DA, dopamine; LD, L-DOPA; MD, methyl L-dopa; CA, catechol; EP, epinephrine; NE, norepinephrine

■ REFERENCES

(1) Li, J.; Zhu, M.; Manning-Bog, A. B.; Di Monte, D. A.; Fink, A. L. Dopamine and L-dopa Disaggregate Amyloid fibrils: Implications for Parkinson's and Alzheimer's Disease. *FASEB J.* **2004**, *18*, 962−964.

(2) Mor, D. E.; Tsika, E.; Mazzulli, J. R.; Gould, N. S.; Kim, H.; Daniels, M. J.; Doshi, S.; Gupta, P.; Grossman, J. L.; Tan, V. X.; Kalb, R. G.; Caldwell, K. A.; Caldwell, G. A.; Wolfe, J. H.; Ischiropoulos, H. Dopamine Induces Soluble Alpha-Synuclein Oligomers and Nigrostriatal Degeneration. *Nat. Neurosci.* **2017**, *20*, 1560−1568.

(3) Velander, P.; Wu, L.; Ray, W. K.; Helm, R. F.; Xu, B. Amylin Amyloid Inhibition by Flavonoid Baicalein: Key Roles of Its Vicinal Dihydroxyl Groups of the Catechol Moiety. *Biochemistry* **2016**, *55*, 4255−4258.

(4) Ono, K.; Hasegawa, K.; Naiki, H.; Yamada, M. Curcumin Has Potent Anti-Amyloidogenic Effects for Alzheimer's Beta-Amyloid Fibrils In Vitro. *J. Neurosci. Res.* **2004**, *75*, 742−750.

(5) Ono, K.; Hasegawa, K.; Naiki, H.; Yamada, M. Anti-Amyloidogenic Activity of Tannic Acid and Its Activity to Destabilize Alzheimer's Beta-Amyloid Fibrils In Vitro. *Biochim. Biophys. Acta* **2004**, *1690*, 193−202.

(6) Ehrnhoefer, D. E.; Bieschke, J.; Boeddrich, A.; Herbst, M.; Masino, L.; Lurz, R.; Engemann, S.; Pastore, A.; Wanker, E. E. EGCG Redirects Amyloidogenic Polypeptides into Unstructured, Off-Pathway Oligomers. *Nat. Struct. Mol. Biol.* **2008**, *15*, 558−566.

(7) Hyung, S.-J.; DeToma, A. S.; Brender, J. R.; Lee, S.; Vivekanandan, S.; Kochi, A.; Choi, J.-S.; Ramamoorthy, A.; Ruotolo, B. T.; Lim, M. H. Insights into Antiamyloidogenic Properties of the Green Tea Extract (−)-Epigallocatechin-3-gallate Toward Metal-Associated Amyloid-β Species. *Proc. Natl. Acad. Sci. U.S.A.* **2013**, *110*, 3743−3748.

(8) Palhano, F. L.; Lee, J.; Grimster, N. P.; Kelly, J. W. Toward the Molecular Mechanism(s) by Which EGCG Treatment Remodels Mature Amyloid Fibrils. *J. Am. Chem. Soc.* **2013**, *135*, 7503−7510.

(9) Makin, S. The Amyloid Hypothesis on Trial. *Nature* **2018**, *559*, S4−S7.

(10) d'Ischia, M.; Napolitano, A.; Pezzella, A.; Meredith, P.; Buehler, M. Melanin Biopolymers: Tailoring Chemical Complexity for Materials Design. *Angew. Chem., Int. Ed.* **2020**, *59*, 11196−11205.

(11) Song, H.; Kim, Y.; Kim, I.; Kim, Y. K.; Kwon, S.; Kang, K. Multifaceted Influences of Melanin-Like Particles on Amyloid-Beta Aggregation. *Chem.—Asian J.* **2020**, *15*, 91−97.

(12) Fowler, D. M.; Koulov, A. V.; Alory-Jost, C.; Marks, M. S.; Balch, W. E.; Kelly, J. W. Functional Amyloid Formation Within Mammalian Tissue. *PLoS Biol.* **2006**, *4*, No. e6.

(13) McGlinchey, R. P.; Shewmaker, F.; McPhie, P.; Monterroso, B.; Thurber, K.; Wickner, R. B. The Repeat Domain of the Melanosome Fibril Protein Pmel17 Forms the Amyloid Core Promoting Melanin Synthesis. *Proc. Natl. Acad. Sci. U.S.A.* **2009**, *106*, 13731−13736.

(14) Watt, B.; van Niel, G.; Fowler, D. M.; Hurbain, I.; Luk, K. C.; Stayrook, S. E.; Lemmon, M. A.; Raposo, G.; Shorter, J.; Kelly, J. W.; Marks, M. S. N-terminal Domains Elicit Formation of Functional Pmel17 Amyloid Fibrils. *J. Biol. Chem.* **2009**, *284*, 35543−35555.

(15) Watt, B.; van Niel, G.; Raposo, G.; Marks, M. S. PMEL: a Pigment Cell-Specific Model for Functional Amyloid Formation. *Pigm. Cell Melanoma Res.* **2013**, *26*, 300−315.

(16) Brunberg, E.; Andersson, L.; Cothran, G.; Sandberg, K.; Mikko, S.; Lindgren, G. A Missense Mutation in PMEL17 is Associated with the Silver Coat Color in the Horse. *BMC Genet.* **2006**, *7*, 46.

(17) Shin, J. H.; Le, N. T. K.; Jang, H.; Lee, T.; Kang, K. Supramolecular Regulation of Polydopamine Formation by Amyloid Fibers. *Chem. - Eur. J.* **2020**, *26*, 5500−5507.

(18) Otzen, D.; Riek, R. Functional Amyloids. *Cold Spring Harbor Perspect. Biol.* **2019**, *11*, a033860.

(19) Lee, B. P.; Messersmith, P. B.; Israelachvili, J. N.; Waite, J. H. Mussel-Inspired Adhesives and Coatings. *Annu. Rev. Mater. Res.* **2011**, *41*, 99−132.

(20) Hong, S.; Wang, Y.; Park, S. Y.; Lee, H. Progressive Fuzzy Cation-π assembly of Biological Catecholamines. *Sci. Adv.* **2018**, *4*, No. eaat7457.

(21) Panzella, L.; Gentile, G.; D'Errico, G.; Della Vecchia, N. F.; Errico, M. E.; Napolitano, A.; Carfagna, C.; d'Ischia, M. Atypical Structural and π -ElectronFeatures of a Melanin Polymer That Lead to Superior Free -Radical-ScavengingProperties. *Angew. Chem., Int. Ed.* **2013**, *52*, 12684−12687.

(22) Hong, S.; Kim, J.; Na, Y. S.; Park, J.; Kim, S.; Singha, K.; Im, G.-I.; Han, D.-K.; Kim, W. J.; Lee, H. Poly(norepinephrine): Ultrasmooth Material-Independent Surface Chemistry and Nanodepot for Nitric Oxide. *Angew. Chem., Int. Ed.* **2013**, *52*, 9187−9191.

(23) Kang, K.; Choi, J.-M.; Fox, J. M.; Snyder, P. W.; Moustakas, D. T.; Whitesides, G. M. Acetylation of Surface Lysine Groups of a Protein Alters the Organization and Composition of Its Crystal Contacts. *J. Phys. Chem. B* **2016**, *120*, 6461−6468.

(24) Sato, M.; Murakami, K.; Uno, M.; Nakagawa, Y.; Katayama, S.; Akagi, K.-i.; Masuda, Y.; Takegoshi, K.; Irie, K. Site-Specific Inhibitory Mechanism for Amyloid β42 Aggregation by Catechol-Type Flavonoids Targeting the Lys Residues. *J. Biol. Chem.* **2013**, *288*, 23212−23224.

(25) Yan, Z.; Yin, M.; Chen, J.; Li, X. Assembly and Substrate Recognition of Curli Biogenesis System. *Nat. Commun.* **2020**, *11*, 241.

(26) Evans, M. L.; Chapman, M. R. Curli Biogenesis: Order Out of Disorder. *Biochim. Biophys. Acta, Mol. Cell Res.* **2014**, *1843*, 1551−1558.

(27) Wang, Y.-h.; Zhang, Y.-g. Amyloid and Immune Homeostasis. *Immunobiology* **2018**, *223*, 288−293.

(28) Salinas, N.; Tayeb-Fligelman, E.; Sammito, M. D.; Bloch, D.; Jelinek, R.; Noy, D.; Usón, I.; Landau, M. The Amphibian Antimicrobial Peptide Uperin 3.5 is a Cross-α/cross-β Chameleon Functional Amyloid. *Proc. Natl. Acad. Sci. U.S.A.* **2021**, *118*, No. e2014442118.

(29) Maji, S. K.; Perrin, M. H.; Sawaya, M. R.; Jessberger, S.; Vadodaria, K.; Rissman, R. A.; Singru, P. S.; Nilsson, K. P. R.; Simon, R.; Schubert, D.; Eisenberg, D.; Rivier, J.; Sawchenko, P.; Vale, W.; Riek, R. Functional Amyloids as Natural Storage of Peptide Hormones in Pituitary Secretory Granules. *Science* **2009**, *325*, 328−332.

(30) Javed, I.; Zhang, Z.; Adamcik, J.; Andrikopoulos, N.; Li, Y.; Otzen, D. E.; Lin, S.; Mezzenga, R.; Davis, T. P.; Ding, F.; Ke, P. C. Accelerated Amyloid Beta Pathogenesis by Bacterial Amyloid FapC. *Adv. Sci.* **2020**, *7*, 2001299.

(31) Huma, Z. e.; Javed, I.; Zhang, Z.; Bilal, H.; Sun, Y.; Hussain, S. Z.; Davis, T. P.; Otzen, D. E.; Landersdorfer, C. B.; Ding, F.; Hussain, I.; Ke, P. C. Nanosilver Mitigates Biofilm Formation via FapC Amyloidosis Inhibition. *Small* **2020**, *16*, 1906674.

https://doi.org/10.1021/acsomega.1c05399
ACS Omega 2022, 7, 773−779